An Ear-Worn Vital Signs Monitor

An Ear-Worn Vital Signs Monitor

David Da He, Eric S. Winokur, *Member, IEEE*, and Charles G. Sodini, *Fellow, IEEE*

***Abstract*—This work presents a wearable vital signs monitor at the ear. The monitor measures the electrocardiogram (ECG), ballistocardiogram (BCG), and photoplethysmogram (PPG) to obtain pre-ejection period (PEP), stroke volume (SV), cardiac output (CO), and pulse transit time (PTT).**

The ear is demonstrated as a natural anchoring point for the integrated sensing of physiological signals. All three signals measured can be used to obtain heart rate. Combining the ECG and BCG allows for the estimation of the PEP, while combining the BCG and PPG allows for the measurement of PTT. Additionally, the J-wave amplitude of the BCG is correlated to the SV, and when combined with HR, yields CO. Results from a clinical human study on 13 subjects demonstrate this proof of concept device.

***Index Terms*—ballistocardiogram, blood pressure, cardiac output, continuous monitoring, electrocardiogram, heart rate, stroke volume, photoplethysmogram, pre-ejection period, pulse transit time**

I. Introduction

CARDIOVASCULAR disease (CVD) affects 37% of the United States population and is the leading cause of death in the U.S. [1]. Many key cardiovascular parameters including heart rate, stroke volume, and the pre-ejection period (PEP) have specific applications in the field of CVD monitoring.

Heart rate can be used to monitor arrhythmias that contain irregular beat intervals. An example is atrial fibrillation, which is the most common form of cardiac arrhythmia and increases the risk of stroke and heart failure [2]. As a measure of the heart's pumping ability, stroke volume is an important parameter for congestive heart failure (CHF) patients. The PEP can be used to evaluate ventricular performance in CHF patients, who have an inability to decrease the PEP upon cardiovascular demand, and are characterized with a prolonged PEP [3].

When stroke volume is multiplied with heart rate, cardiac output can be obtained, which is defined as the total volume of blood pumped per minute. Because of the heart's reduced pumping ability, CHF patients exhibit decreased cardiac output [3].

Manuscript received January 31, 2015, accepted on July 17, 2015. This work was sponsored by the Medical Electronic Device Realization Center (MEDRC) at MIT. Human subject testing was conducted at the MIT Catalyst Clinical Research Center under IRB approval #1104004449, CRC protocol #615, and grant #UL1 RR025758.

E. S. Winokur, D. He, and C. G. Sodini are with the Department of Electrical Engineering and Computer Science, Massachusetts Institute of Technology, Cambridge, MA, 02139 (e-mail: ewinokur@mit.edu; david.he@alum.mit.edu; sodini@mit.edu).

This work uses the site behind the ear as a measurement location. Physiologically, we show that several signals can be measured at the ear location. These signals include the ballistocardiogram (BCG), the electrocardiogram (ECG), and the photoplethysmogram (PPG). Mechanically, the mastoid area behind the ear is rigid, which reduces motion artifacts compared to peripheral locations such as the earlobe and the finger. The ear location is discreet because a small device can be concealed by the ear or hair. Furthermore, as demonstrated by hearing aids and headsets, the ear acts as a natural anchor, allowing device attachment using an ear bud instead of adhesives.

The monitor has been tested on 13 healthy subjects in a clinic to verify measured data with clinical grade instrumentation. The proof-of-concept monitor measures the BCG, ECG, and PPG and estimates HR, PEP, SV, CO, and PTT. This paper is a culmination of our previous work [4] [5] [6] [7], with additional results showing a new method for obtaining SV from head BCG. Further studies should be conducted to validate our device on CVD patients.

II. Background

The BCG is a non-invasive measurement of the body's mechanical recoil to the blood ejected by the heart during systole. Early work demonstrated that the BCG morphology offers insight into stroke volume, the risk of heart attack, and mortality [8] [9]. Recently, there is a renewed interest in the BCG [10] [11] [12]. All of these methods involve a stationary measurement device for non-ambulatory monitoring.

To avoid ECG wires from the ear-worn device to the chest, we measure the ECG locally near the ear. The ECG near the ear is significantly attenuated and only R-waves are visible. However, this is sufficient for calculating the RJ interval, which is defined as the interval between the ECG's R-wave and the BCG's J-wave [13] [14] and has high correlation to the heart's pre-ejection period [15] [16]. PEP can be used to determine left ventricular performance in patients with CVD such as cardiomyopathy and abnormal left ventricular contractions [17] [18].

The photoplethysmogram is generally measured at the finger to maximize signal quality and is usually used to estimate blood oxygenation [19]. We measure the photoplethysmogram behind the ear at the mastoid above Reid's Baseline. Obtaining heart rate from the BCG, ECG and PPG signals can be used for redundancy error checking to ensure high signal quality.

III. Methods

A. Measuring the Head Ballistocardiogram

To sense the head BCG, we use a 14-bit low noise MEMS

tri-axial accelerometer (Bosch BMA180 with 150μG/rtHz noise) that is mounted at the ear. All BCG signals are bandpass filtered from 1Hz to 10Hz to remove the gravity contribution and higher frequency artifacts.

Fig. 1 shows that the head BCG in the upright standing posture exists in all three axes. The y-axis (headward-footward) is the dominant BCG axis because the blood volume movement is mainly in the y-axis.

To examine the secondary BCG waves, the ensemble average of the head BCG is created by aligning each beat's J-wave and then averaging the beats. As shown in Fig. 2, the H, I, K, and L-waves become visible in the ensemble average.

Because the head BCG is in the range of 10mG, it can only be measured in states of relative rest. However, for the target application of long term wearable monitoring, numerous measurement periods exist throughout the day when the wearer is at less than 4mG of acceleration [16].

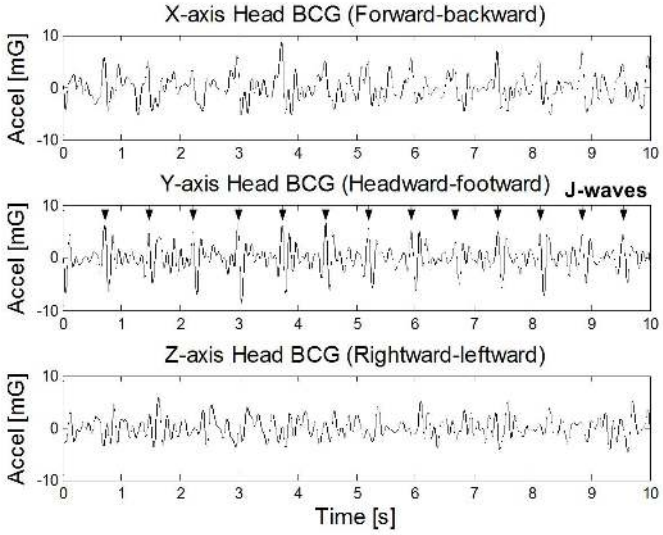

Fig. 1. Measured tri-axial head BCG in the standing posture with J-waves annotated in the y-axis data.

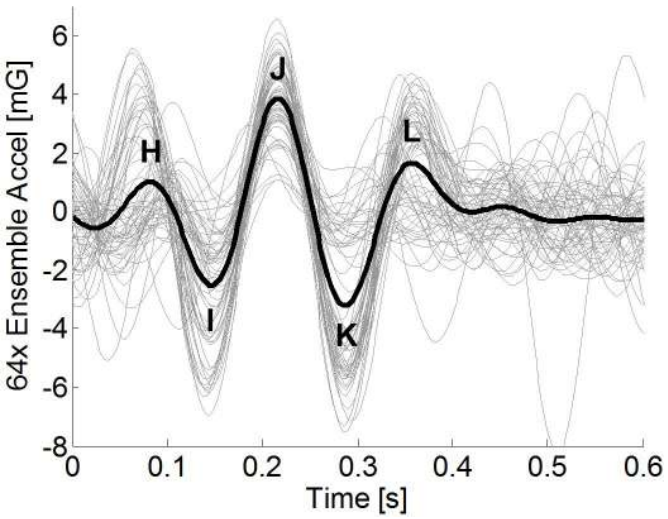

Fig. 2. The ensemble head BCG from 64 beats where the underlying individual BCG waveforms are shown in gray.

B. Measuring the Head Electrocardiogram

To sense the ECG at the head, one electrode is placed on the mastoid area, and the second electrode is placed on the posterior upper middle neck. The mastoid's bony structure and the neck's flat surface provide a stable electrode contact. Together, the two electrodes measure a single-lead ECG.

Usually, a third driven-right-leg (DRL) electrode is used for common-mode interference rejection as well as feedback to set the DC potential of the body. However, this DRL electrode is omitted because of the limited area near the ear. As a result, a digital filter removes powerline interference. The ECG front-end circuit is shown in Fig. 3.

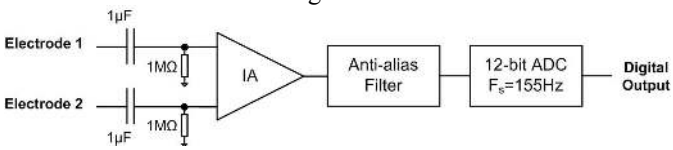

Fig. 3. The head ECG front-end circuit.

Using AgCl gel electrodes, Fig. 4 shows ECG measurements taken from the chest (lead II, 15cm apart, gain of 250) and from the left mastoid area (4cm apart, gain of 7,000).

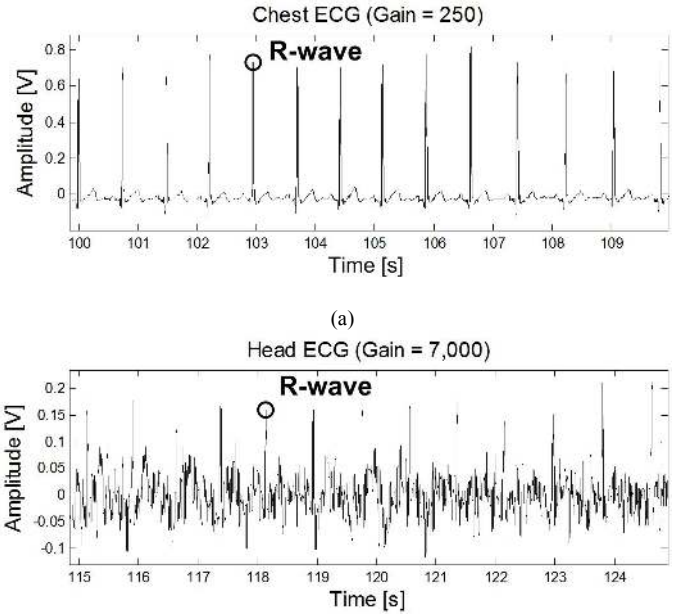

Fig. 4. a) The ECG measured from the chest, and b) the ECG measured from the mastoid area behind the left ear. The measurements are not simultaneous.

As seen in Fig. 4, the ECG measured at the mastoid area is in the range of $30\mu V_{pp}$, which is two orders of magnitude less than the standard chest ECG. This attenuation is due to the pattern of the ECG field lines at the head, which yield a very small potential difference when projected onto the mastoid lead. Because of this attenuation, the head ECG has a poor signal-to-noise ratio and only R-waves are immediately visible.

C. Extracting the RJ Interval

To extract the RJ interval, the simplest method is to use a peak detection algorithm to determine the delay between the ECG's R-wave and the BCG's J-wave. However, as shown in Fig. 5 (a), the BCG and the ECG signals at the head have low signal-to-noise ratios where a peak detection algorithm is prone to error.

Instead, cross-correlation is proposed as a noise tolerant method for determining the RJ interval. This method takes advantage of the fact that both head BCG and head ECG waveforms have a similar morphology and are phase-locked to a lag index equal to the RJ interval.

To demonstrate this, Fig. 5(b) shows a time segment of the head ECG signal cross-correlated with a simultaneous head BCG signal. The highest peak of the cross-correlation result occurs when the ECG's R-wave and the BCG's J-wave coincide during time-shifting. As expected, the lag index of the highest cross-correlation peak is the RJ interval.

To reduce the amount of computation, the cross-correlation can be limited to a lag range of 0.1s to 0.3s because the RJ interval is physiologically within this range [21]. This range is shown as the shaded region in Fig. 5(b). For example, if the time window is 8s long, then this 0.2s truncation allows a 97.5% computational saving compared to a complete cross-correlation. Another benefit of this truncation is that it removes nearby cross-correlation peaks from consideration, thus improving peak confidence. In the clinical test analysis, a window length of 8s is chosen to reliably extract the RJ intervals.

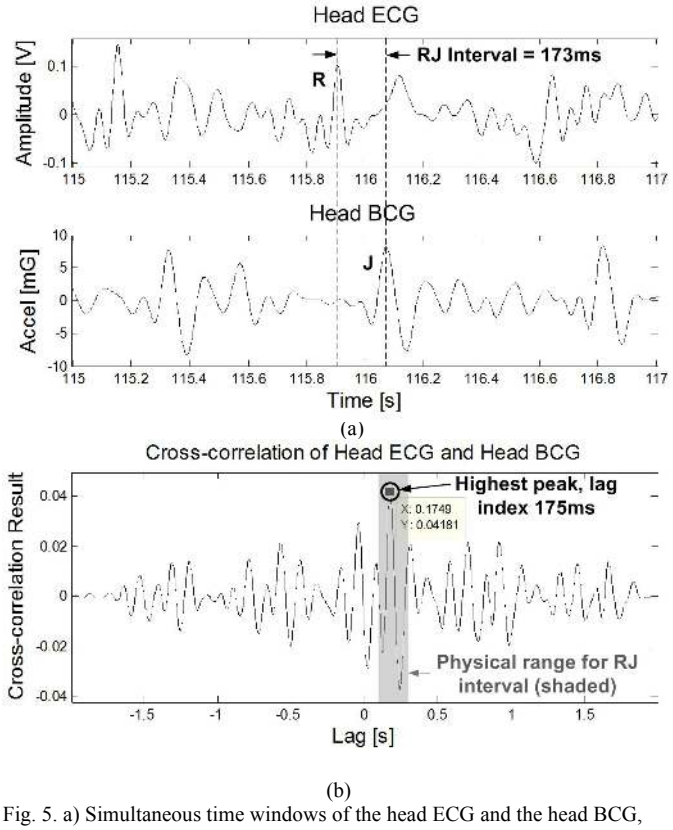

Fig. 5. a) Simultaneous time windows of the head ECG and the head BCG, and b) the cross-correlation result showing that the highest peak's lag index is the RJ interval.

D. Measuring the Head Photoplethysmogram

PPG signals at the head are obtained with a sensor operating in reflectance-mode instead of transmission-mode. In reflectance-mode, the LEDs shine light into the body, and the backscattered light from tissue, blood and bone is received by photodiodes in the same plane as the LED. Several new challenges arise in reflectance-mode PPG. First, the mechanical housing of the sensor may not be sufficient for blocking ambient light from the PDs, therefore, care must be taken when sampling and filtering to avoid aliasing interferers into the PPG bandwidth of interest. Second, reflectance-mode measurements are often part of wearable systems, which require low-power and low-voltage operation to reduce the battery size and optimize the form factor. To help mitigate these issues, the wearable vital signs monitor uses a dynamic range enhancement (DRE) circuit to lower the voltage of the PPG front end and reduce the resolution requirements of the analog-to-digital converter (ADC) [7] [20].

Head PPG signals are similar to PPG signals obtained by transmission through the finger, as shown by Fig. 6. The morphological differences are due to the vascular transmission line, which sends the pulse from the heart to the head, compared to the finger.

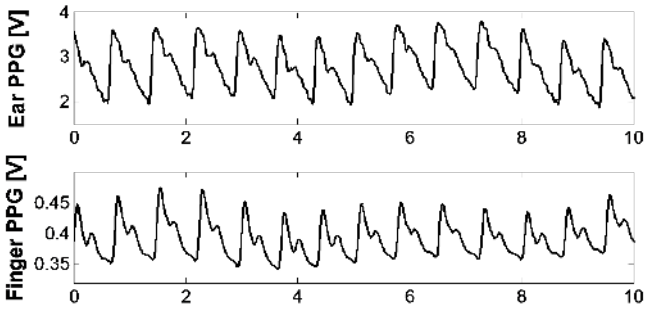

Fig. 6. Top: PPG taken from the mastoid region behind the left ear. Bottom: PPG taken from the finger.

E. Device Design

The wearable device measures the BCG and the ECG at the head and sends the data wirelessly to a computer for visualization, recording, and analysis. The device is shown in Fig. 7 and the system block diagram is shown in Fig. 8.

The microcontroller (MSP430) continuously samples the BCG and the ECG sensors at 155Hz and sends the data to a 2.4GHz low power wireless transceiver (CC2500). The power management circuit draws power from a single 3V 220mAh lithium coin cell battery (CR2032). The computer interface consists of a CC2500 transceiver and a MSP430 microcontroller, which sends the received data to the computer's USB port. The computer records, plots, and filters the BCG and the ECG data in real time using MATLAB.

A modified hearing aid housing manufactured by Taising Hearing Amplifier Ltd mechanically supports the PCB's. The device is anchored to the ear using the attached earbud. Two ECG electrodes are attached to the mastoid and the neck using AgCl gel electrodes. Table I contains the important system parameters.

F. Failure Cases

The ear-worn vital signs monitor measures signals with low SNR, such as the ballistocardiogram. In order to obtain measurements that are uncorrupted, the user should be relatively sedentary. If the user is moving, then the data is unusable. To avoid reporting erroneous data, the accelerometer could be used to detect when the user is sedentary and then take the physiological measurements. Previous studies have shown that users have several windows throughout the day where acceleration is less than 4mG [16].

Additionally, checking that all three physiological signals measure the same heart rate can also be used to ensure that the data is not corrupted.

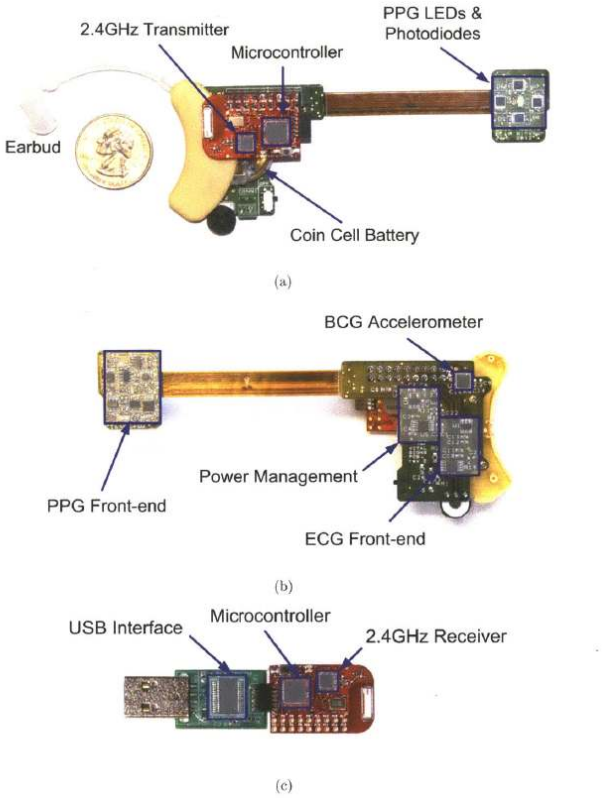

Fig. 7. The wearable measurement hardware for single-site, continuous PTT measurements along the carotid artery. Figure from [7].

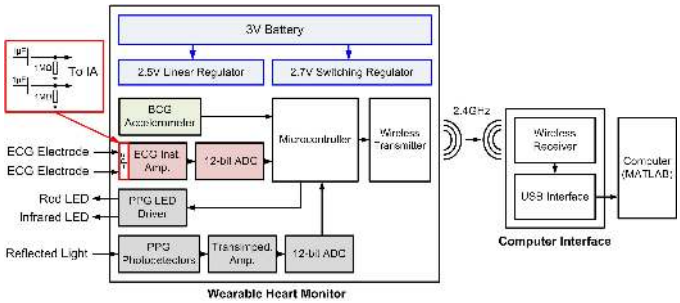

Fig. 8. The system block diagram of the wearable vital signs monitor with arrows indicating the signal paths.

G. Human Subjects Study

Clinical testing was conducted at MIT's Clinical Research Center (CRC), and the protocol was approved by MIT's Institutional Review Board (IRB). The protocol begins by consenting a subject, followed by a health questionnaire to ensure the subject had no prior cardiovascular conditions. Reference equipment was then attached to the subject, which included a Criticare 504-US chest ECG (lead II configuration) and finger pulse oximeter, a Sonosite BioZ Dx impedance cardiography (ICG) machine for measuring pre-ejection period (PEP) and cardiac output (CO), and a Finapres Portapres for continuous blood pressure measurements.

TABLE I
SYSTEM PARAMETERS

Parameter	Value
System Power	30 mW (after LDO)
Accel noise	0.47 mG RMS
ECG AFE noise	0.16μV RMS
PPG AFE noise	4.3nA RMS

Instrumentation was completed when the wearable vital signs monitor was attached to the left ear of the subject.

The test was performed on 13 healthy subjects, consisting of 10 male subjects and three female subjects. The subjects varied from 25 years old to 63 years old (mean 39.7, std 14.2), 1.55m to 1.93m in height (mean 1.77m, std 0.097m), and 49.9kg to 103kg in weight (mean 74.8kg, std 12.9kg). Figure 9 shows a screen shot of the wearable monitor collecting data simultaneously for a single user.

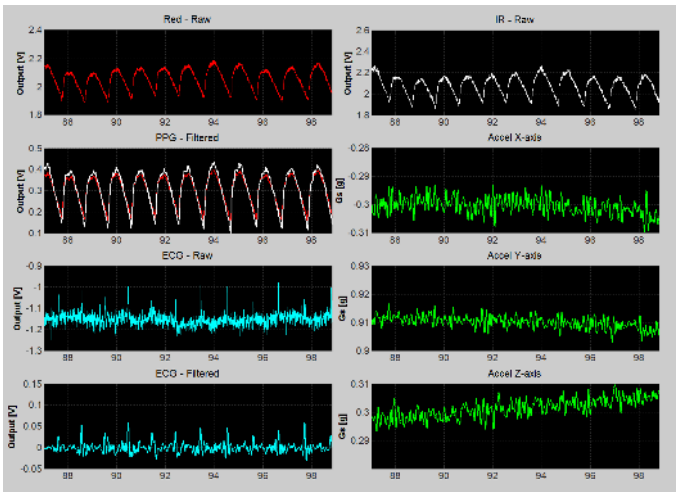

Fig. 9. A screen shot of the data collected by the wearable vital signs monitor. From top to bottom, left to right: raw red PPG, filtered red and IR PPG, raw ECG, filtered ECG, raw IR PPG, accelerometer X axis, accelerometer Y axis, and accelerometer Z axis.

IV. HUMAN SUBJECT STUDY RESULTS AND DISCUSSION

A. Stroke Volume

J-wave amplitudes are extracted from 20-beat ensemble averages in the standing posture from each subject. Fig. 10 plots J-wave amplitudes versus stroke volumes from 13 subjects. A linearly proportional relationship between J-wave amplitudes and stroke volumes is observed because the BCG recoil is directly related to the mass (or volume) of the pumped blood.

It is important to note that our study was limited to healthy patients, who did not have vessel diseases that could confound the BCG to SV results. A larger study is required to assess the overall BCG to SV relationship. Nevertheless, our data showed an R^2 correlation of 0.66.

B. The Pre-ejection Period

The Valsalva maneuver is designed to induce a temporary increase in the subjects' PEP. The RJ interval is extracted by cross-correlating the wearable device's BCG and ECG, while

the reference PEP is measured using the ICG machine.

Fig. 11 shows an example of measured RJ interval and PEP from a subject who performs a Valsalva maneuver from 43s to 63s. The decreased venous return and ventricular filling volume during Valsalva lead to a prolonged PEP. The PEP's increase of 30*ms* corresponds to an equal increase in the RJ interval during the strain.

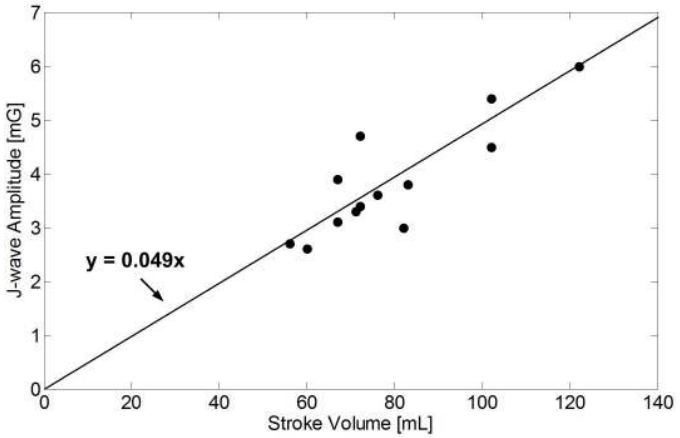

Fig. 10. J-wave amplitudes (from device) versus stroke volumes (from ICG). Each data point is one subject.

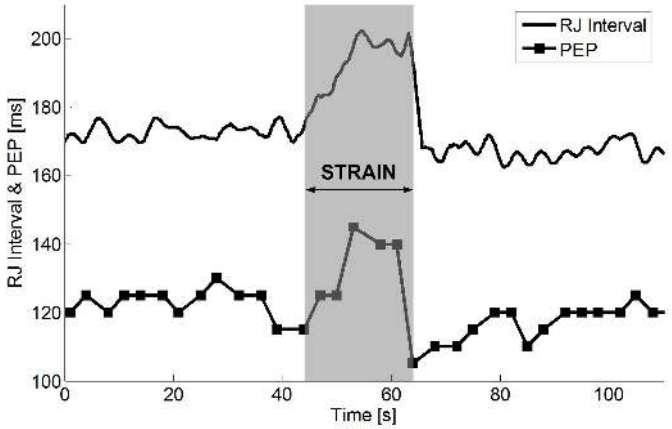

Fig. 11. Simultaneously measured RJ interval (from device) and PEP (from ICG) during a Valsalva maneuver.

It is observed that the RJ interval is always longer than the PEP by an offset duration that is subject dependent. This is because the opening of the aortic valve marks the end of the PEP, while the J-wave occurs when the blood is accelerating after exiting the heart. This offset is affected by variables such as body height and blood pressure, thus making it subject dependent.

Fig. 12 plots the beat-to-beat RJ interval versus the PEP after removing the subject-dependent RJ interval-PEP offsets. The data consists of 28 tilt maneuvers from seven subjects with 2,258 beats. The remaining six subjects had faulty PEP measurements, as the ICG machine was unable to detect aortic valve openings. From the data, we observe that the RJ interval exhibits a nearly one-to-one linear dependence on the PEP with a slope of 0.96 and an R^2 value of 0.96.

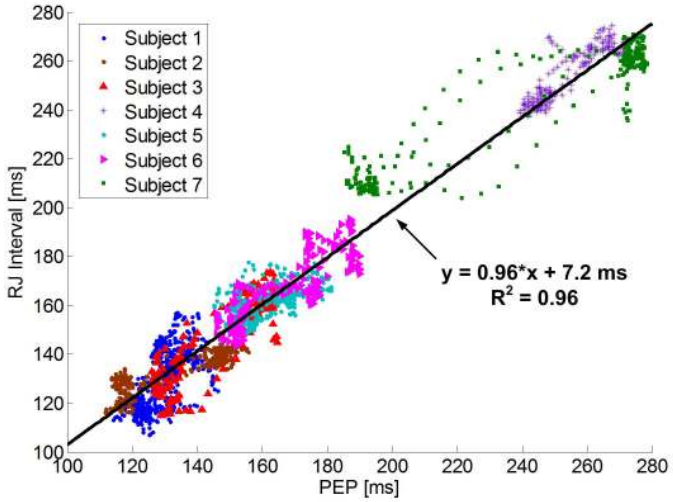

Fig. 12. The beat-to-beat RJ interval (from device) and PEP (from ICG) among seven subjects during 28 tilt maneuvers.

A Bland-Altman representation of the data is shown in Fig. 13, where the standard deviation in differences between the beat-to-beat RJ interval and PEP is 9.6ms for seven subjects.

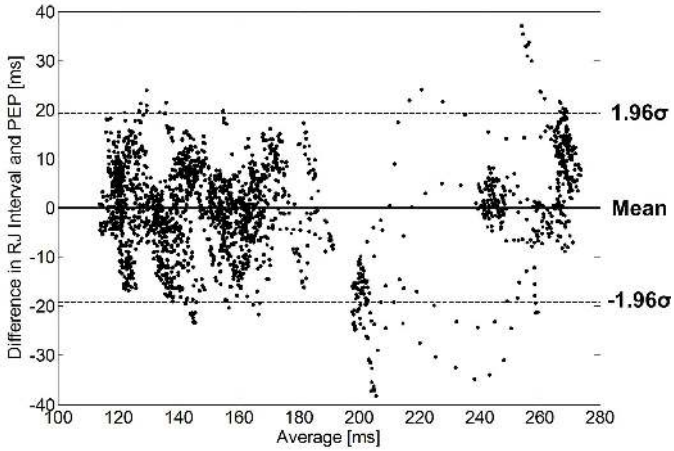

Fig. 13. The Bland-Altman representation of the beat-to-beat RJ interval and PEP from the same data set used in Fig. 12.

C. Utilizing the Ballistocardiogram for PTT Measurements

It has been documented that the PEP is a large error source when estimating blood pressure from transit time measurements [22]. Compared to measurements that use the R-wave of the ECG to the peak of the derivative of the PPG, called pulse arrival time (PAT), PTT using the J-wave of the BCG removes the PEP from the measurement. This increases the accuracy of PTT-to-BP algorithms as the PEP is not constant and does not always correspond appropriately to changes in pressure [7] [22].

V. Conclusions

This work has identified periodic head movements as a type of BCG, which is shown to closely resemble the traditional BCG waveform after ensemble averaging. One direct application of the head BCG is electrode-less heart rate monitoring. Another application is the estimation of stroke volume based on the BCG amplitude. When the BCG is used in conjunction with the ECG, the RJ interval can be extracted

using cross-correlation and is shown to linearly correlate with the PEP. When the BCG is used in conjunction with the PPG, PTT can be measured, which is theoretically correlated to blood pressure.

ACKNOWLEDGMENT

The authors would like to acknowledge Professor Collin Stultz (MIT), Professor Roger Mark (MIT), and Professor Thomas Heldt (MIT) for their valuable physiological discussions and Tom O'Dwyer (Analog Devices) for his insight. The authors would also like to thank nurses Catherine Ricciardi and Ilene Horvitz for their assistance with the clinical test.

REFERENCES

[1] P. Heidenreich et al., "Forecasting the future of cardiovascular disease in the united states: a policy statement from the american heart association," Circulation, vol. 123, pp. 933–944, 2011.

[2] J. Waktare, "Atrial fibrillation," Circulation, vol. 106, no. 1, pp. 14–16, 2002.

[3] A. Weissler, W. Harris, and C. Schoenfeld, "Systolic time intervals in heart failure in man," Circulation, vol. 37, no. 2, pp. 149–159, 1968.

[4] He, D.D, et al., "The ear as a location for wearable vital signs monitoring," *Engineering in Medicine and Biology Society (EMBC), 2010 Annual International Conference of the IEEE* , vol., no., pp.6389,6392, Aug. 31 2010-Sept. 4 2010.

[5] He, D.D.; Winokur, E.S.; Sodini, C.G., "A continuous, wearable, and wireless heart monitor using head ballistocardiogram (BCG) and head electrocardiogram (ECG)," *Engineering in Medicine and Biology Society, EMBC, 2011 Annual International Conference of the IEEE* , vol., no., pp.4729,4732, Aug. 30 2011-Sept. 3 2011.

[6] He, D.D.; Winokur, E.S.; Sodini, C.G., "An ear-worn continuous ballistocardiogram (BCG) sensor for cardiovascular monitoring," *Engineering in Medicine and Biology Society (EMBC), 2012 Annual International Conference of the IEEE* , vol., no., pp.5030,5033, Aug. 28 2012-Sept. 1 2012.

[7] E. Winokur, D. He, and C. Sodini, "A Wearable Vital Signs Monitor at the Ear for Coninuous Heart Rate and Pulse Transit Time Measurements," *IEEE EMBC*, pp. 2724-2727, 2012.

[8] H. Mandelbaum and R. Mandelbaum, "Studies utilizing the portable electromagnetic ballistocardiograph: Iv. the clinical significance of serial ballistocardiograms following acute myocardial infarction," Circulation, vol. 7, pp. 910–915, 1953.

[9] I. Starr and F. Wood, "Twenty-year studies with the ballistocardiograph: The relation between the amplitude of the first record of healthy adults and eventual mortality and morbidity from heart disease," Circulation, vol. 23, pp. 714–732, 1961.

[10] O. Inan et al., "Robust ballistocardiogram acquisition for home monitoring," Physiological Measurement, vol. 30, no. 2, p. 169, 2009.

[11] K. Kim et al., "A new method for unconstrained pulse arrival time (pat) measurement on a chair," J. Biomed. Eng. Res., vol. 27, pp. 83–88, 2006.

[12] G. Chung et al., "Wakefulness estimation only using ballistocardiogram: Nonintrusive method for sleep monitoring," in IEEE Engineering in Medicine and Biology Conference, 2010, pp. 2459–2462.

[13] J. Shin, K. Lee, and K. Park, "Non-constrained monitoring of systolic blood pressure on a weighing scale," Physiological Measurement, vol. 30, no. 7, p. 679, 2009.

[14] A. Weissler, *Noninvasive Cardiology*. New York, NY, USA: Grune and Stratton, Inc., 1974.

[15] C. G. Jr., A. Weissler, and H. Dodge, "The relationship of alterations in systolic time intervals to ejection fraction in patients with cardiac disease," Circulation, vol. 42, pp. 455–462, 1970.

[16] M. D. Rienzo et al., "24h seismocardiogram monitoring in ambulant subjects," in IEEE Engineering in Medicine and Biology Conference, 2012, pp. 5050–5053.

[17] W. Chen and D. Gibson, "Mechanisms of prolongation of pre-ejection period in patients with left ventricular disease," Br. Heart J., vol. 42, pp. 304–310, 1979.

[18] M. Etemadi et al., "Non-invasive assessment of cardiac contractility on a weighing scale," in IEEE Engineering in Medicine and Biology Conference, 2009, pp. 6773–6776.

[19] J. G. Webster, Design of Pulse Oximeters. Bristol, PA, USA: Philadelphia: Institute of Physics Pub., 1997, Medical Science Series.

[20] E. S. Winokur, T. O'Dwyer and C. G. Sodini, "A Low-Power, Dual-Wavelength Photoplethysmogram (PPG) SoC With Static and Time-Varying Interferer Removal," *IEEE TBioCAS*, accepted for publishing.

[21] L. Giovangrandi, et al., "Preliminary Results from BCG and ECG Measurements in the Heart Failure Clinic," *IEEE EMBC*, San Diego, CA, 2012, pp. 3780 – 3783.

[22] R. Payne, C. Symeonides, D. Webb, and S. Maxwell, "Pulse transit time measured from the ECG: an unreliable marker of beat-to-beat blood pressure," J. Appl. Physiol., vol. 100, no. 1, pp. 136-141, Sep. 2006.

David Da He received the B.A.Sc. degree in electrical engineering from the University of Toronto in 2005, and the S.M. and the Ph.D. degrees in electrical engineering from the Massachusetts Institute of Technology, in 2008 and 2013, respectively.

Dr. He has worked on a variety of sensors, including cardiovascular monitors, an organic thin-film transistor temperature sensor, and industrial wireless condition monitoring sensors. He has served on the technical committee of the IEEE International Conference on Body Sensor Networks, and is recognized as one of MIT Technology Review's 35 Innovators Under 35 in 2014.

Currently, Dr. He is a co-founder and the Chief Scientific Officer of Quanttus, where he works on new ways for wearable sensors, algorithms, and data insights to transform how we view personal health.

Eric S. Winokur (M '07) received the B.S. and M.S. degree in electrical engineering from Lehigh University, Bethlehem, PA in 2006 and 2008 respectively, and the Ph.D. degree from the Massachusetts Institute of Technology in 2014, Cambridge, MA.

He was an intern at Texas Instruments' Kilby Labs, in 2010. His research interests include non-invasive cardiovascular monitoring, wearable sensors, integrated circuit design, and physiology.

Dr. Winokur was a recipient of the 2010 ADI Outstanding Student Designer Award, was a Sherman Fairchild Fellow at Lehigh University, is a member of Phi Beta Pi, and was a winner of Lehigh University's Student Entrepreneurship Competition in 2006.

Charles G. Sodini received the B.S.E.E. degree from Purdue University, in 1974, and the M.S.E.E. and the Ph.D. degrees from the University of California, Berkeley, in 1981 and 1982, respectively. He was a member of the technical staff at Hewlett-Packard Laboratories from 1974 to 1982, where he worked on the design of MOS memory. He joined the faculty of the Massachusetts Institute of Technology, in 1983, where he is

currently the LeBel Professor of Electrical Engineering. His research interests are focused on medical electronic systems for monitoring and imaging. These systems require state-of-the-art mixed signal integrated circuit and systems with extremely low energy dissipation. He is the co-founder of the Medical Electronic Device Realization Center at MIT.

Along with Prof. Roger T. Howe, he is a co-author of an undergraduate text on integrated circuits and devices entitled "Microelectronics: An Integrated Approach." He also studied the Hong Kong/South China electronics industry in 1996-97 and has continued to study the globalization of the electronics industry.

Dr. Sodini was a co-founder of SMaL Camera Technologies, a leader in imaging technology for consumer digital still cameras and machine vision cameras for automotive applications. He has served on a variety of IEEE Conference Committees, including the International Electron Device Meeting where he was the 1989 General Chairman. He has served on the IEEE Electron Device Society Administrative Committee and was president of the IEEE Solid-State Circuits Society from 2002-2004. He was the Chair of the Executive Committee for the VLSI Symposia from 2007-2014 and a Fellow of the IEEE.